ORNL/TM-10392

ornl

OAK RIDGE NATIONAL LABORATORY

MARTIN MARIETTA

Computer Simulation of Absorption Heat Pump Using Aqueous Lithium Bromide and Ternary Nitrate Mixtures

Moonis R. Ally

OPERATED BY
MARTIN MARIETTA ENERGY SYSTEMS, INC.
FOR THE UNITED STATES
DEPARTMENT OF ENERGY

Printed in the United States of America. Available from
National Technical Information Service
U.S. Department of Commerce
5285 Port Royal Road, Springfield, Virginia 22161
NTIS price codes—Printed Copy: A04; Microfiche A01

ORNL/TM-10392

Energy Division

COMPUTER SIMULATION OF ABSORPTION HEAT PUMP USING AQUEOUS LITHIUM BROMIDE AND TERNARY NITRATE MIXTURES

Moonis R. Ally

Date Published

June 1988

OAK RIDGE NATIONAL LABORATORY
Oak Ridge, Tennessee 37831
operated by
MARTIN MARIETTA ENERGY SYSTEMS, INC.
for the
Office of Industrial Programs
U.S. DEPARTMENT OF ENERGY
under Contract DE-AC05-840R21400

CONTENTS

LIST OF FIGURES

ACKNOWLEDGMENTS

Appreciation is expressed to Mr. Stephen Kaplan, Mr. Bob Chappell, Mr. Scott Richlen, and Dr. Gershon Grossman (Haifa Technion University) for their support and help. Appreciation is also expressed to Gil Farrell for typing the manuscript, LeRoy Gilliam for doing the art work, and Sharon McConathy, Eleanor Rogers, and E. W. Whitfield for their editorial skills.

The document was prepared for the U.S. Department of Energy, Office of Industrial Programs.

EXECUTIVE SUMMARY

This report presents the results of a computer simulation study aimed at comparing the potential performance of lithium bromide (LiBr) and ternary nitrate aqueous mixtures in a temperature amplifier heat pump.

In this study, the falling film heat transfer coefficient for the ternary nitrate mixture is estimated to be lower than that for LiBr by about one-third. Due to a lack of measured thermophysical properties, the estimates relied on extrapolations.

The results show that the ternary nitrate mixture may be operated up to 260°C (500°F) boost temperature, which is approximately 80°C (176°F) higher than what has been demonstrated with LiBr. In higher temperature regimes, the nitrates show the potential for 10% higher COPs and a marginally greater absorber capacity than LiBr.

Experimental measurements of the falling film heat transfer coefficient, subcooling, and thermophysical properties are required to make a more definitive investigation.

ABSTRACT

A new aqueous ternary mixture consisting of 53 wt % $LiNO_3$, 28 wt % KNO_3, and 19 wt % $NaNO_3$ is available for high-temperature heat pump applications. The pressure-composition-temperature and the specific enthalpy-concentration-temperature data in the form of correlated polynomial expressions are used in a computer program to simulate results of a temperature amplifier heat pump with $LiBr/H_2O$ and ternary nitrate/H_2O mixtures as working fluids. Although the limits of applicability of the two fluids are different, there is a region of commonality where the comparison can be made. The difficulty is a lack of adequate thermophysical data on both mixtures in the temperature ranges of interest. In the absence of adequate thermophysical data for the fluids, the study serves as a best guess first approximation. The results show that the ternary nitrate mixture potentially has approximately a 10% advantage in COP and a 15% advantage in temperature lifts over aqueous LiBr at high temperatures. Ternary nitrates are hampered by crystallization at low waste heat temperatures and cannot operate competitively in the low lift and waste heat temperature regions. The potential performance advantage at high temperatures for the ternary nitrate mixture is sufficiently attractive to justify additional work to obtain adequate thermodynamic transport and corrosion data.

1. INTRODUCTION

Ternary mixtures, serving as working fluids, are reported[1,2] to help improve the coefficient of performance (COP) or temperature-lift capabilities of heat-actuated heat pumps. Some well-known ternary mixtures are $NH_3/H_2O/LiBr$, $CH_3NH_2/H_2O/LiBr$, and $CH_3OH/LiBr/ZnBr_2$. A recent development[3] in ternary mixtures is an aqueous mixture of 53 wt % $LiNO_3$, 28 wt % KNO_3, and 19 wt % $NaNO_3$, henceforth referred to as ternary nitrate mixture (TNM). This new fluid is potentially a competitor to existing chemical heat pump fluids and operates up to 260°C (500°F).

This report compares the potential performance of the ternary nitrate and lithium bromide (LiBr) aqueous mixtures in a computer simulation of a temperature amplifier heat pump.

2. WORKING MEDIA PROPERTIES

The pressure-composition-temperature (P-X-T) and the specific enthalpy-composition-temperature (H-X-T) data for the working fluids are critical pieces of information for heat pump cycle calculations. In the case of LiBr aqueous mixtures, these thermodynamic properties are well documented between 50 and 350°F.[4] The specific enthalpies of pure refrigerant (water) and steam are available in steam tables. In the case of the ternary nitrate mixtures, Ally[5] has represented the experimental P-X-T and H-X-T data by polynomial equations similar in form to the ones published for LiBr in the ASHRAE Handbook of Fundamentals.[4] These equations for LiBr and TNMs will be shown later with their attendant Duhring and specific enthalpy plots. The main facility provided by these equations is that they can easily be incorporated in a computer program.

2.1 EQUATIONS DESCRIBING P-X-T AND H-X-T DATA

The P-X-T data for TNMs and LiBr mixtures are superimposed on one another in Fig. 1. The relationship between the saturation temperature of the pure refrigerant (pure water in each case) and the temperature of the mixture of known concentration, X (wt %), can be represented for either working fluid by an equation of the form,

$$t = A(X)t' + B(X) \quad , \tag{1}$$

where t and t′ are the mixture and pure refrigerant saturation temperatures expressed in degrees Fahrenheit, respectively, and A and B are polynomial functions of the concentration, X. Of course, the functional dependence of A and B on X will be different for the two mixtures as is seen by their respective expressions in Fig. 1. The equilibrium vapor pressure of water above the mixture is given by a van't Hoff type of equation,

$$\mathrm{Log}_{10}P = C + \frac{D}{(t' + 459.67)} + \frac{E}{(t' + 459.67)^2} \quad , \tag{2}$$

where C, D, and E are constants that must be the same for both mixtures because they share a common refrigerant between them. The reasons why Eq. (2) is used for both LiBr and TNMs are explained in detail elsewhere.[5]

EQUILIBRIUM CHART FOR AQUEOUS LITHIUM BROMIDE AND TERNARY MIXTURES

TERNARY SALT COMPOSITION

53 wt % $LiNO_3$
28 wt % KNO_3
19 wt % $NaNo_3$

$t = At' + B$

$A = -1.06 + 0.1021X - 1.627 \times 10^{-3}X^2 + 8.931 \times 10^{-6}X^3$

$B = 291.1 - 13.03X + 0.1871X^2 - 7.877 \times 10^{-4}X^3$

$$\log P = C + \frac{D}{(t' + 459.67)} + \frac{E}{(t' + 459.67)^2}$$

X = wt % TERNARY SALT

P = psia

$50 \leq X \leq 94.1$

$32 \leq t' \leq 450$

LITHIUM BROMIDE MIXTURE

$t = At' + B$

$t' = (t - B)/A$

$A = -2.00755 + 0.16976X - (3.133362E-3)X^2 + (1.97668E-5)X^3$

$B = 321.128 - 19.322X + 0.374382X^2 - (2.0637E-3)X^3$

$\log_{10} P = C + D/(t' + 459.72) + E/(t' + 459.72)^2$

$$t' = \frac{-2E}{D + [2 - 4E(C - \log_{10} P)]^{0.5}} - 459.72$$

TEMPERATURE RANGE	
REFRIGERANT	$0 \leq t' \leq 230°F$
SOLUTION	$0 \leq t \leq 350°F$
CONCENTRATION RANGE	$45\% \leq X \leq 70\%$

$C = 6.21147$
$D = -2886.373$
$E = -337269.46$
t' = REFRIGERANT TEMPERATURE (°F)
t = SOLUTION TEMPERATURE (°F)
X = PERCENT ABSORBENT
P = psia

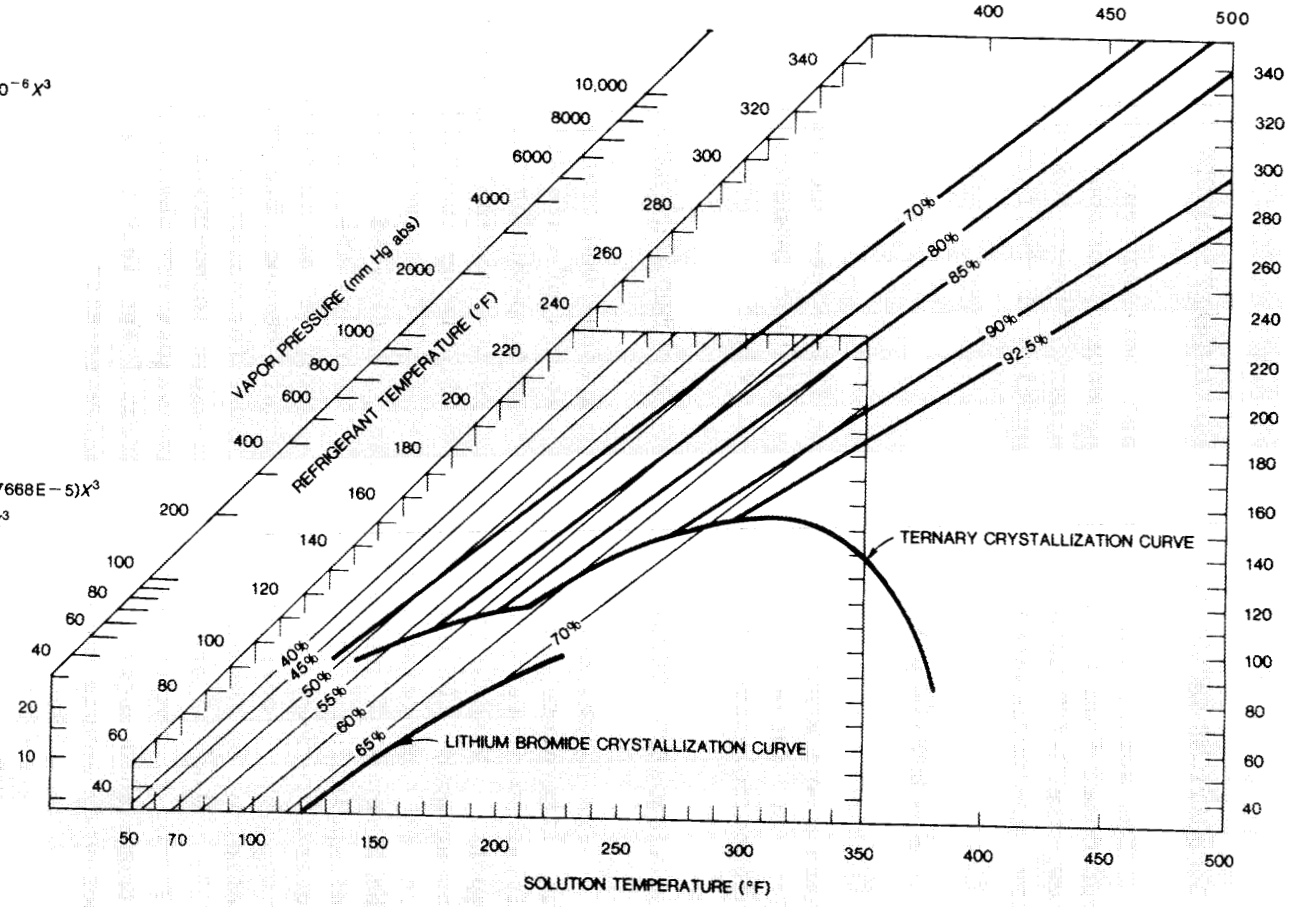

Fig. 1. Pressure-composition-temperature data (Duhring chart) for aqueous LiBr and ternary nitrate mixtures.

2.2 EQUATIONS DESCRIBING SPECIFIC ENTHALPY-CONCENTRATION DATA

The specific H-X-T data and correlations for aqueous LiBr are reproduced from the ASHRAE Fundamentals Handbook[4] in Fig. 2a. Figure 2b shows the H-X-T data for the ternary nitrate mixture. The experimental data[3] are correlated with an equation of the form,

$$H = \alpha(X) + \beta(X)t \ , \tag{3}$$

where α and β are polynomials in the solute (ternary salt) concentration, X (wt %), and t is the solution temperature. Details regarding this correlation are reported in ref. 5.

2.3 VISCOSITY, SPECIFIC GRAVITY, AND THERMAL CONDUCTIVITY DATA

The narrow scope of thermophysical and transport data available in the literature and the sparse amounts of data available for the ternary nitrate mixture were a serious handicap during the preparation of this report. Viscosity, specific gravity, thermal conductivity, etc., data for aqueous LiBr mixtures are available up to 100°C (212°F), but properties at temperatures up to 180°C (356°F) were needed for this study. In the absence of experimental data, estimated values were obtained by extrapolation (Figs. 2c,d,e). Perhaps the only source of data for the aqueous ternary nitrate fluid is ref. 3, which contains adequate data on viscosity, lacks considerable data on specific gravity, and is severely deficient on thermal conductivity, for which only two values of 0.31 and 0.33 $W/m^2 \cdot K$ are quoted at salt concentrations of 86.7 wt % and 83.7 wt %, respectively. These values are themselves obtained through a recommended power law equation.[3] The lack of specific gravity data is not very severe because thermal expansion,

$$-\frac{1}{V}\left(\frac{\partial V}{\partial T}\right)_P \ ,$$

is small over the temperature range of interest. But the error on thermal conductivity could deviate substantially from the estimated value of 0.31 to 0.33 $W/m^2 \cdot K$.

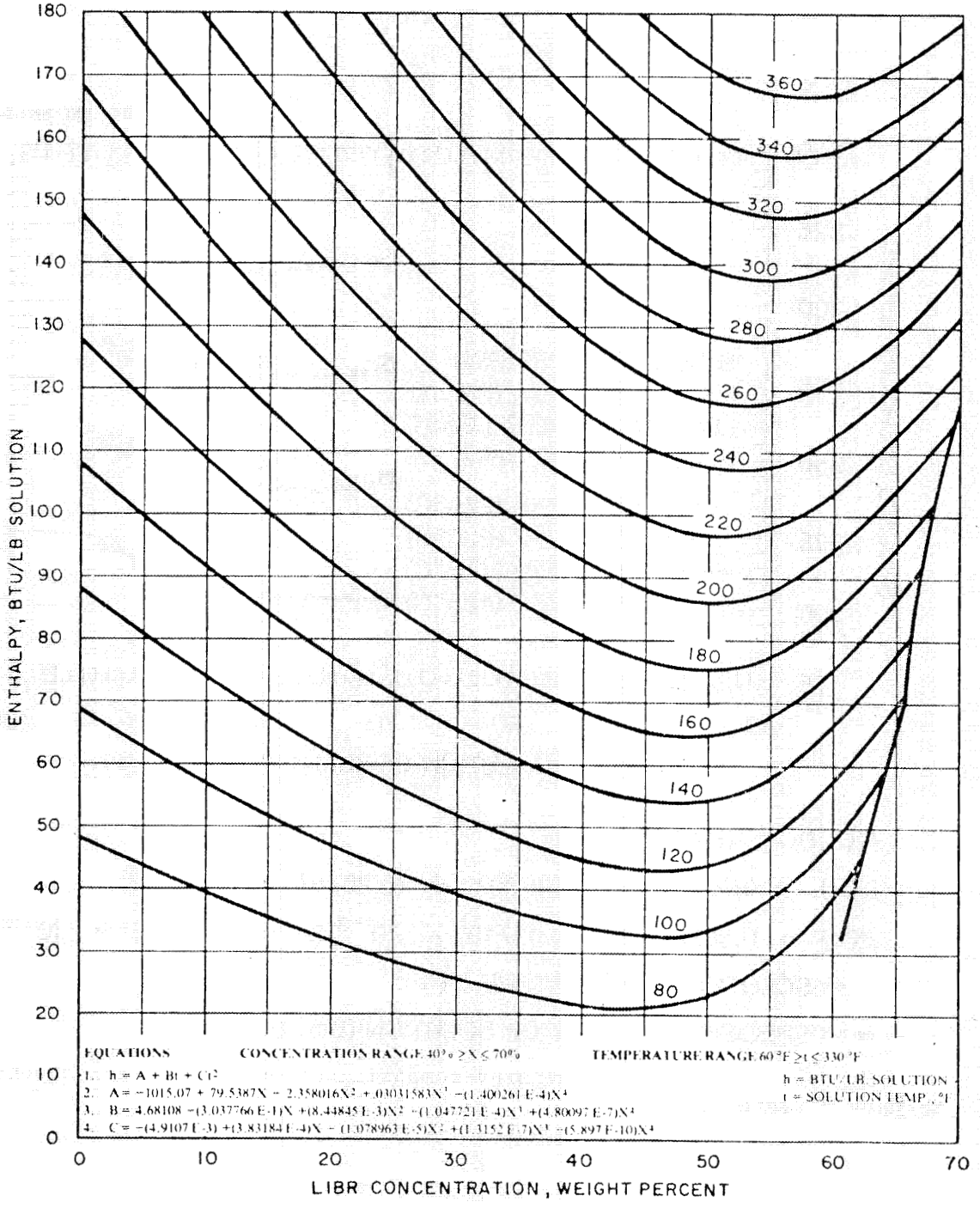

Fig. 2. (*a*) Specific enthalpy-composition-temperature for lithium bromide-water mixtures.

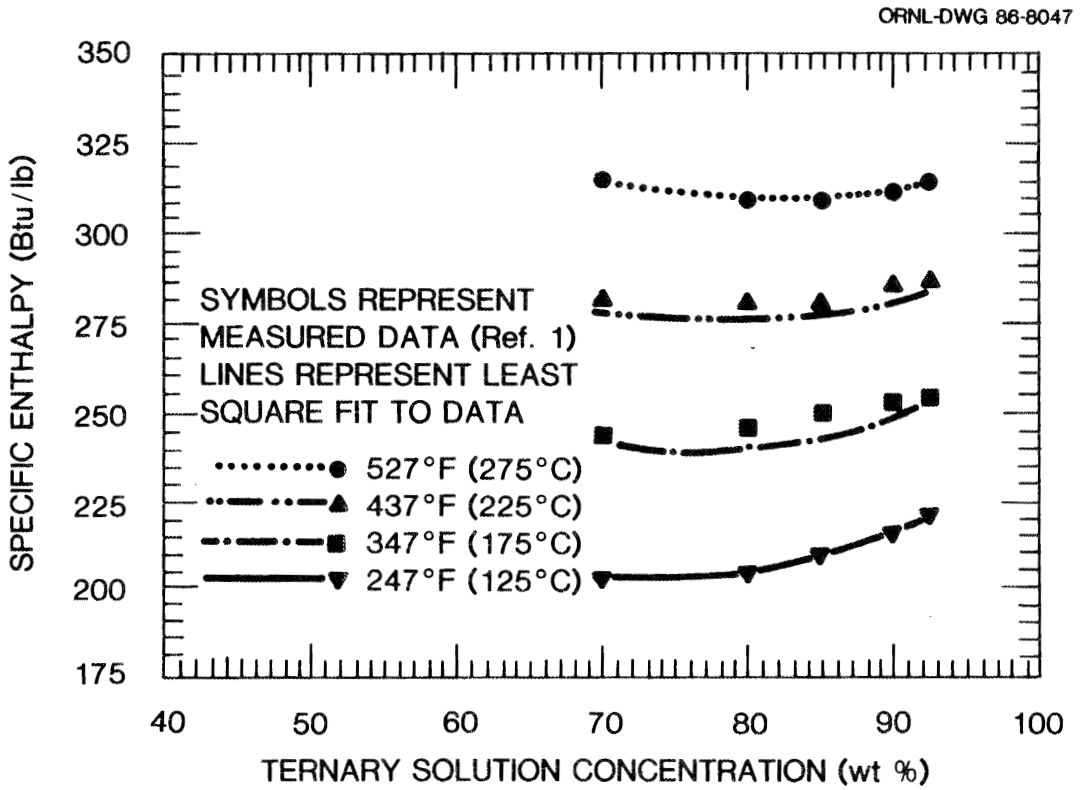

$$H(X,t) = \alpha(X) + \beta(X)t$$

$$\alpha(X) = 394.516 - 8.64996X + (6.28787 \times 10^{-2})X^2$$

$$\beta(X) = 0.388691 + (3.02719 \times 10^{-3})X - (3.80068 \times 10^{-5})X^2$$

t = SOLUTION TEMPERATURE (°F)

H = SPECIFIC ENTHALPY OF SOLUTION (Btu/lb)

Fig. 2. (*b*) Specific enthalpy-composition-temperature for aqueous ternary nitrate mixtures.

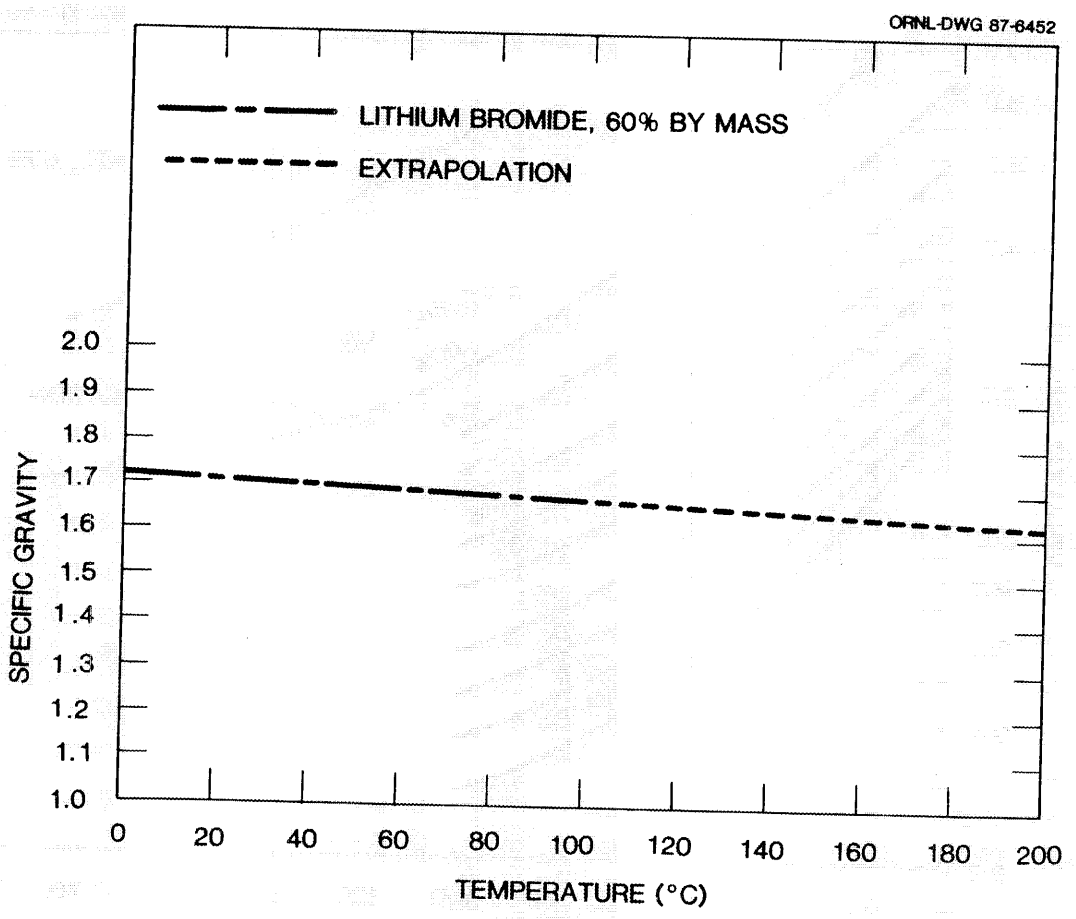

Fig. 2. (c) Specific gravity for LiBr.

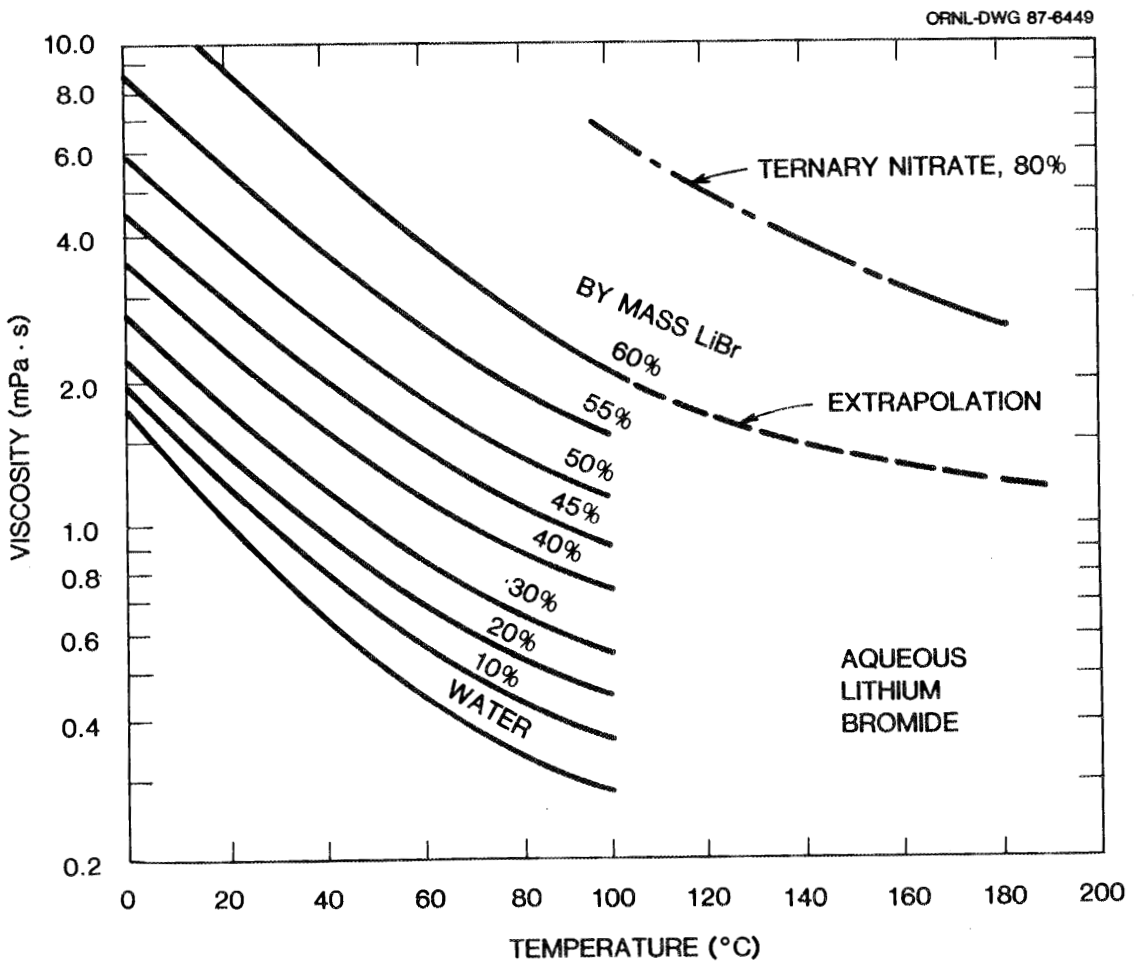

Fig. 2. (*d*) Viscosity of LiBr and ternary nitrate mixture.

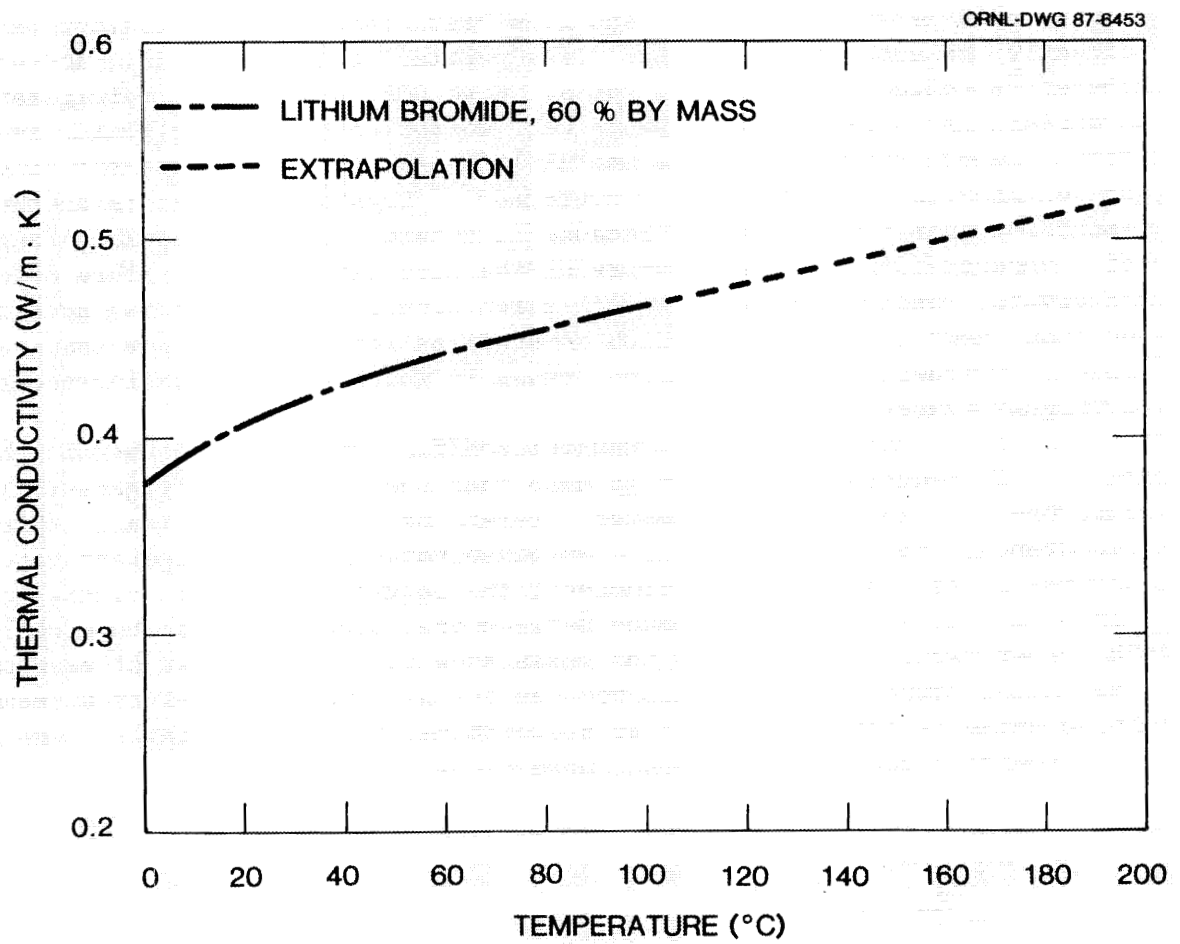

Fig. 2. (*e*) Thermal conductivity of LiBr mixtures.

3. COMPUTER SIMULATION

Operation of a single-stage temperature amplifier heat pump was simulated using a program developed by Grossman and Michelson.[6]

The criteria for evaluating absorption fluids from a practical standpoint are (a) the coefficient of performance, (b) the temperature lift and boost temperatures, (c) the flow rates of refrigerant, (d) potential corrosion problems, (e) crystallization limits, (f) film heat transfer coefficients, (g) mass transfer rate of sorbate into sorbent, and (h) HX area per unit capacity. The coefficient of performance, refrigerant flow rates, and film heat transfer coefficient are directly related to the size of a particular heat pump unit and are therefore reflected in capital costs. High COP, heat, and refrigerant transfer rates reduce heat pump size. Corrosion by working fluids is a strong determinant of hardware useful life expectancy, and its reduction or elimination is obviously preferred. Crystallization is another important operating parameter because it determines the acceptable range of concentration and temperature of the circulating fluid before onset of crystallization. Once crystallization occurs, the system may have to be shut down. Mixtures in which crystallization occurs at low temperatures are generally preferred over those in which crystallization occurs at higher temperatures.

First, consider the heat transfer coefficient. The absorber is the focus of attention because it is here that the sorbate (refrigerant) is absorbed into the sorbent, thereby releasing heat. At least three resistances to heat transfer are involved between the refrigerant vapor and the process stream being produced, the largest of which is resistance due to the film resistance between the sorbent and the tube wall. The other two resistances are the resistance to heat transfer offered by the metal tube wall and that between the wall and the utility stream. These three resistances in series are combined to yield a single overall heat transfer coefficient, U_o as shown below,

$$U_o = \frac{1}{\frac{D_o}{D_i h_i} + \frac{x_w}{k_m}\frac{D_o}{\bar{D}_L} + \frac{1}{h_o}},$$

where D_o and D_i are the outside and inside diameters of the tube, x_w is the tube wall thickness, k_m is the metal thermal conductivity, $\bar{D}_L$ is the logarithm mean diameter of the tube, and h_o is the film heat transfer coefficient. The term, $\frac{1}{h_o}$ represents the resistance to heat transfer

offered by the sorbent film around the absorber tubes, and its magnitude is greater than the magnitude of the first two terms in the denominator in the above equation. For this reason, the film heat transfer coefficient is called "limiting" because it has a dominant influence on U_o and limits its value close to the value of h_o.

A large value of h_o is desirable because it implies a low film heat transfer resistance. Typically, film heat transfer coefficients have a value of 2000 $W/m^2 \cdot K$ and a value greater than this number would be advantageous because the absorber would require less surface area for a given capacity. Conversely, a value lower than 2000 $W/m^2 \cdot K$ would be disadvantageous because of higher heat exchanger surface area requirements.

The determination of heat transfer coefficients is beyond the scope of this simulation study because they must be determined experimentally to be of value to the designer. Therefore, for the simulation study, the same value of film heat transfer coefficient was used for the LiBr and ternary nitrate fluids for a first-cut approximation. Then, on the basis of established theory[7] where mass and heat transfer are decoupled, the film heat transfer coefficient is estimated using experimental and extrapolated data. The details of this procedure are given in the Appendix. Due to the viscosity, density, and thermal conductivity effects, the film heat transfer coefficient for the ternary nitrates is estimated to be about half that for LiBr solutions. The simulation is repeated using the overall heat transfer coefficient for the ternary nitrate taken as one-half that for LiBr, and a third set of simulation considers the scenario where the overall heat transfer coefficient is equal to one-third.

The mass transfer coefficient is a measure of the rate at which the refrigerant is absorbed by the absorbent. If this rate is low, then during the time the refrigerant is in contact with the absorbent, the amount absorbed will be lower than the equilibrium value. As an example, suppose that the solution entering the absorber has 65 wt % salt and pure refrigerant from the evaporator is brought into contact with it. If the rate of mass transfer is rapid, then equilibrium can be reached quickly during the time that the absorbent and refrigerant spend in the absorber. Suppose this equilibrium concentration is 60 wt % salt. If the rate of mass transfer is slow, then equilibrium will not be attained and the quantity of refrigerant absorbed will be less than the equilibrium amount, resulting in a solution with 63 wt % salt. At the same absorber pressure, each of the two solution (equilibrium and actual) concentrations correspond to different temperatures on the Duhring chart, and their difference is known as subcooling. Subcooling is a convenient way to express the departure from equilibrium conditions. From the Appendix, LiBr solutions have viscosities typically of the magnitude of 1.5 mPa·s, while for ternary nitrates, the value is 2.5 mPa·s. In LiBr solutions, experiments show that subcooling is about 2°C when using an effective heat transfer additive for low-pressure absorbers as used in type I absorption chillers. Without an effective

additive, LiBr mixtures typically have 10°C or greater subcooling for low-pressure absorbers. Due to lack of experimental data, the extent of subcooling cannot be quantified; but as explained above, sorbates of higher viscosities will absorb sorbents slower than those having lower viscosities.

Based on the potential COP and temperature lifts shown in Fig. 3, 10°C of subcooling for the ternary nitrate is approximately equal to the advantage that this fluid has over lithium bromide in terms of temperature lift capability.

Since actual heat, mass transfer, and subcooling data are not yet available for the ternary nitrates and since the computer model used in this study does not account for any subcooling, the simplifying assumption of no subcooling for the ternary nitrate and LiBr mixtures is used.

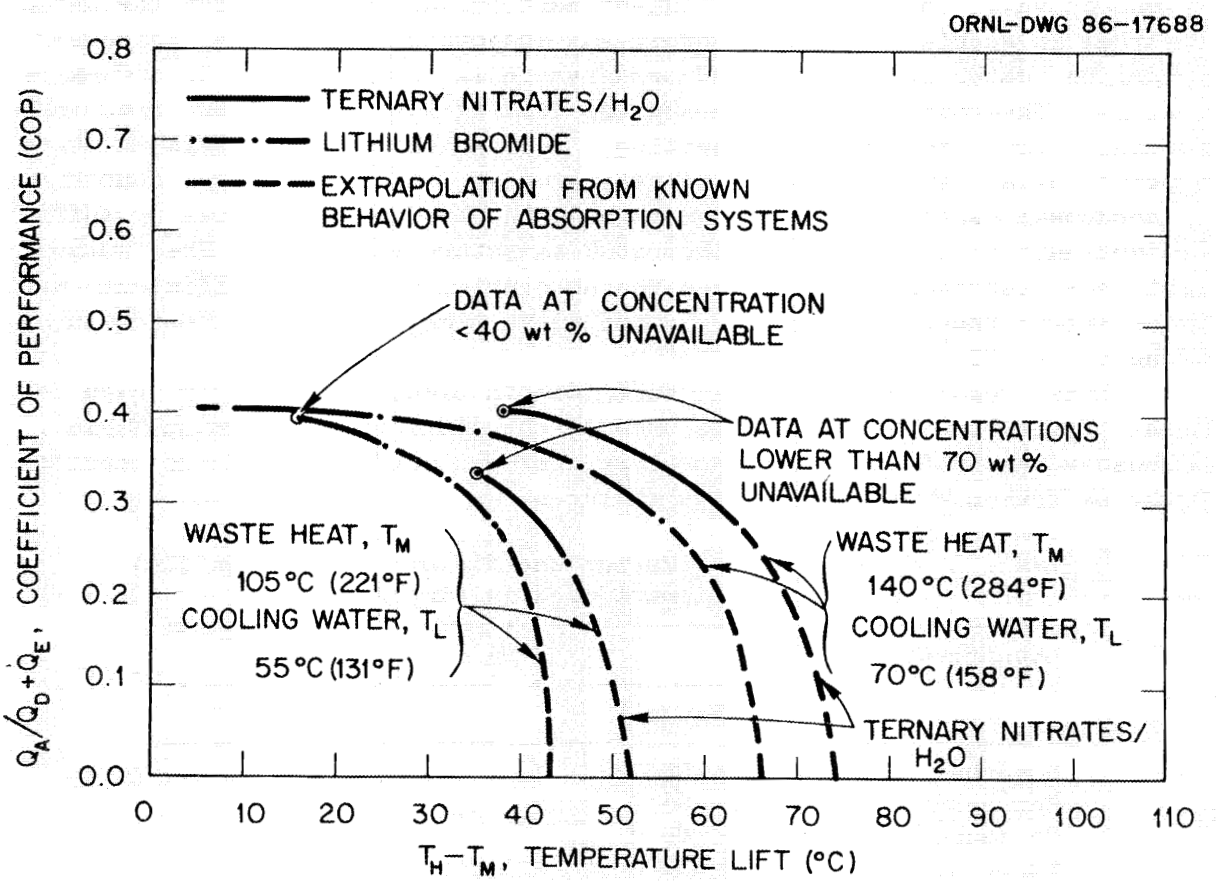

Fig. 3. COP-lift comparison between LiBr and ternary nitrate mixtures.

4. RESULTS

A schematic of the single-stage temperature amplifier heat pump considered for the simulation study is shown in Fig. 4. The waste heat source input to the desorber and evaporator at positions 10 and 1, respectively, is steam at a prescribed (input) temperature. This waste heat source temperature is an input parameter in the program which can arbitrarily be changed. The waste heat streams leaving the desorber and evaporator at positions 11 and 2, respectively, is saturated water at the same pressure as their respective inlet streams. Therefore, no pressure gradient is assumed between state points 10 and 11 and 1 and 2, respectively, and all the latent heat of vaporization from the waste stream is supplied to the desorber and evaporator. In the condenser, cooling water at a prescribed temperature is introduced at 13 and exits at 14. The temperature at 13 and the cooling water mass flow rate are fixed. In the absorber section, the process stream enters at state point 3 at a prescribed temperature at its saturated condition (condensed water). As it goes through the absorber, it picks up sufficient heat to leave the absorber at 9 as saturated steam. The purpose of the recuperator is to make the absorption cycle more efficient, and the effectiveness of the recuperator plays a major role in determining the cycle COP.[8]

The overall heat transfer coefficients times area (UA) in each of the five primary equipments used in the simulation appear in Table 1. These were obtained from a prototype test unit at ORNL used to monitor the performance of LiBr aqueous mixtures.

Table 1. Overall heat transfer coefficient times area (UA) for each equipment used in simulation

Equipment	UA	
	Btu/m°F	W/K x 10^{-3}
Desorber	166.7	5.27
Recuperator	83.3	2.634
Condenser	500	15.81
Evaporator	833	26.34
Absorber	216.7 → 108.3 → 72.2	6.852 → 3.43 → 2.28

A cursory inspection of Fig. 1 shows that there is a small region of overlap between LiBr and ternary mixture solutions. At temperatures below 65°C (≈150°F), the TNMs will certainly present crystallization problems, but LiBr is still suitable for heat pump applications without imminent threat of crystallization. It is believed that LiBr/H_2O may be used at higher temperatures and concentrations than have been reported.

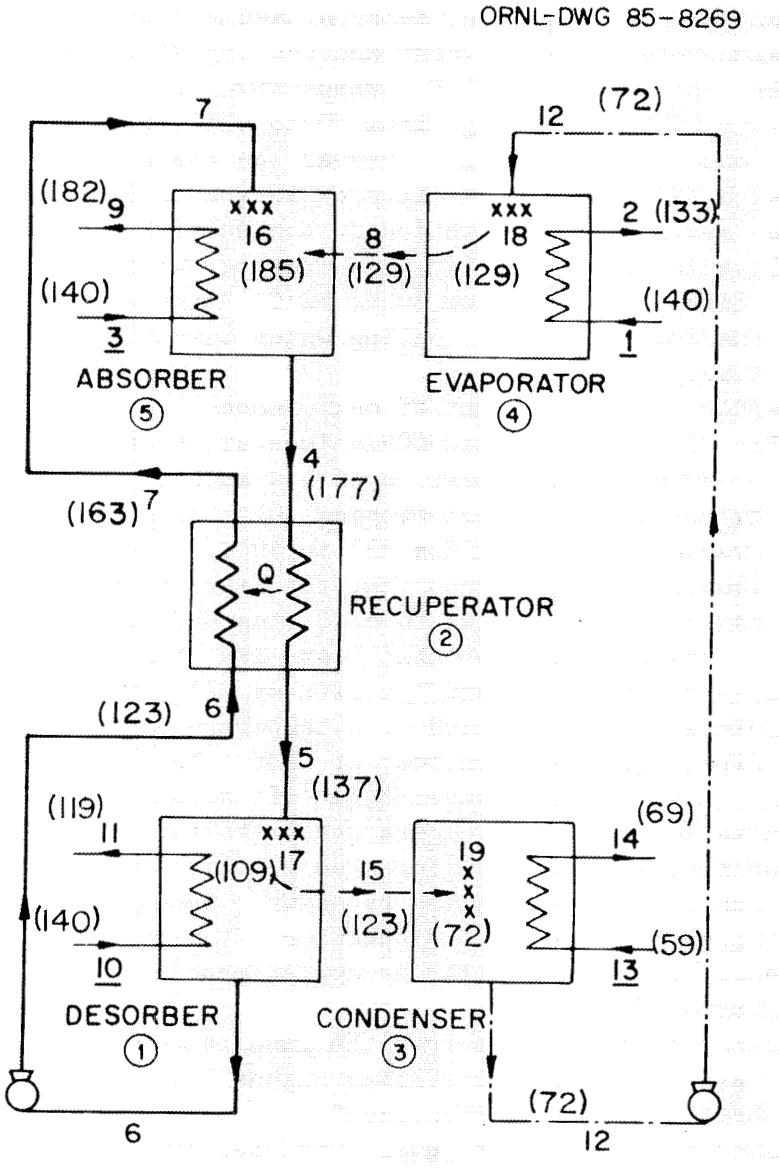

Fig. 4. Schematic representation of the simulated single-stage temperature heat pump with numbered state points.

4.1 COMPARISON BETWEEN LiBr AND TNM WITH EQUAL ABSORBER UA

The computer simulated performances of LiBr and TNMs for two sets of waste heat and cooling water temperatures are shown in Fig. 3. Consider the case where the waste heat and cooling water temperatures are 105°C (221°F) and 55°C (131°F), respectively, and the absorber UA is 6852 W/K. With LiBr, one can go from 10 to 42°C lifts because the concentrations and crystallization curves on the Duhring chart (Fig. 1) allow it. With TNMs, the lower lifts of less than 34°C are not possible because the smallest concentration in the Duhring plot is 70 wt %, and the crystallization curve is very near. Hence, with TNMs the range of temperature lifts varies from 34 to 52°C. Similar arguments apply to the case of the waste heat and cooling water temperatures being 140 and 70°C, respectively.

Considering the coefficient of performance, a comparison of the curves in Fig. 3 shows that the COP values are higher for TNM than they are for LiBr. However, the question of how much of an advantage in COP is afforded by the TNM over LiBr becomes quite ambiguous as the temperature lift is varied. At low lifts (37 to 40°C), the predicted COP of the TNM is about 10% higher than that for LiBr, assuming no subcooling. As the lift is increased from 42 to 52°C, the COP for the LiBr mixture drops off to zero; whereas that for TNM keeps decreasing but is, nevertheless, a finite value until a lift of 52°C, when it too becomes zero. Therefore, between 42 and 52°C temperature lift, the COPs of the TNM are infinitely greater than that of LiBr. The culprit is the precipitous fall in COP with temperature lift because ΔC approaches zero. Therefore, a valid region of temperature lifts for comparison of COPs for the two fluids is one ranging from low lifts up to the point where the precipitous fall in COP begins to occur. Based on the simulation study and in light of the above discussion, it may be appropriate to say that the predicted COP of the TNM is approximately 10% higher than that for LiBr mixtures.

Two further queries arise from the results shown in Fig. 3. They are (i) why are the temperature lifts higher for TNMs? and (ii) why are the COPs higher than they are for LiBr?

The answer to the first query is fairly straightforward. In Fig. 1, the slope of the equilibrium vapor pressure versus solution temperature plot is flatter for the TNMs than those for LiBr, and this flatness helps to reach out further in the solution temperature field. From the Duhring chart, it is an easy matter to determine the maximum boost temperature possible ($\Delta C = 0$) for a given waste heat and cooling water temperature. This information is shown in Fig. 5. It can be seen from Fig. 5 that in the common operating temperature regimes, the temperature boost and, consequently, the temperature lift of the TNMs are potentially greater than they are for LiBr mixtures.

The second question, relating to higher COPs for the TNMs, does not seem to have an overtly obvious answer. Since the definition of COP is $Q_A/Q_D + Q_E$, higher COP values clearly indicate higher numerator values

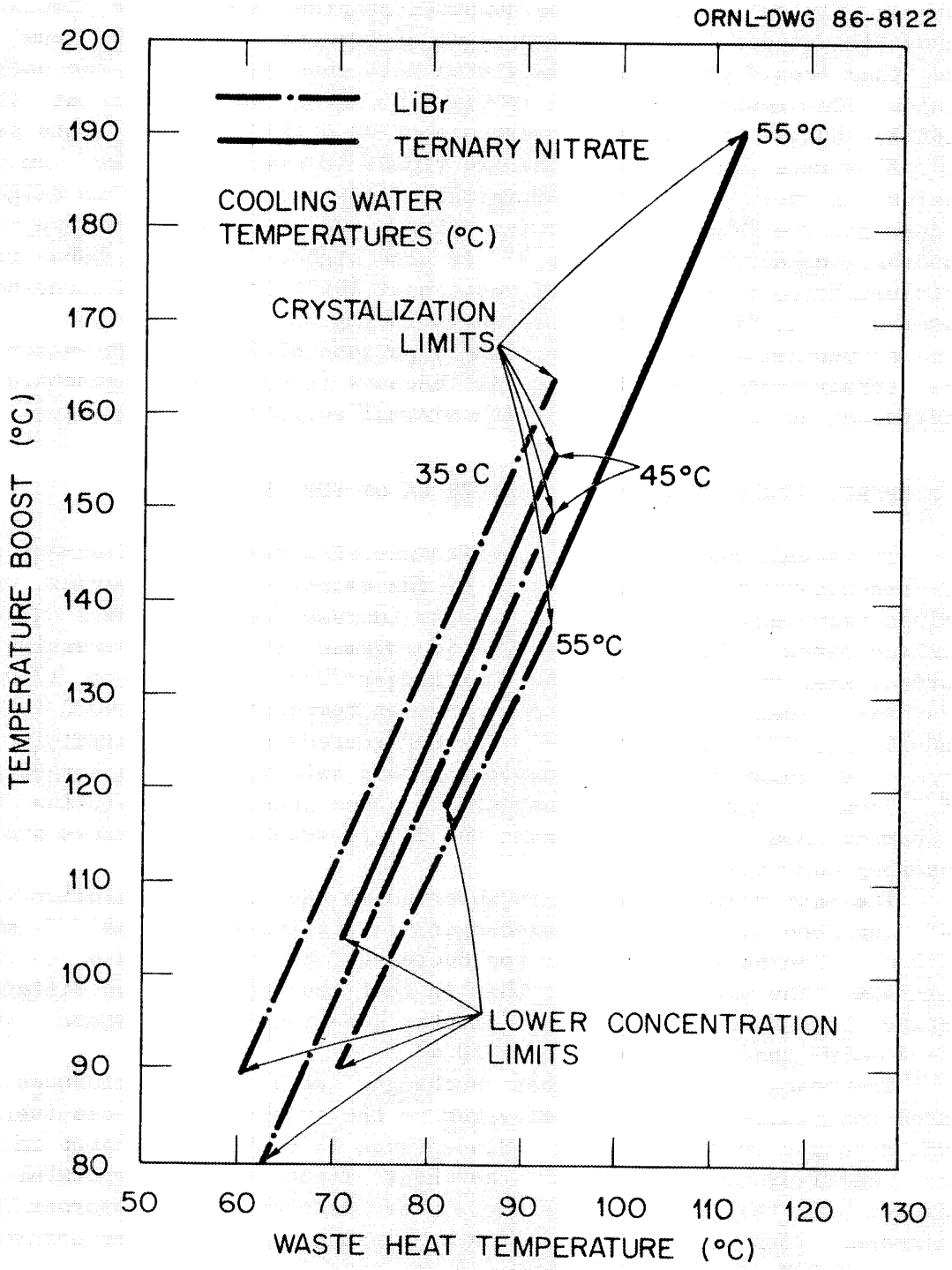

Fig. 5. Temperature boost as a function of waste heat and cooling water temperature for LiBr and ternary nitrate mixtures.

with respect to the denominator, $Q_D + Q_E$. If the values of $Q_D + Q_E$ could be held constant, then the higher COP values are associated with higher Q_A values. Then one could investigate the factors affecting Q_A and from there be able to draw definite conclusions regarding the two working fluids. However, the computer program[6] used in the simulation study did not permit the desired level of freedom in fixing Q_D and Q_E, and they could only approximately be held constant for the two working fluids. The results are shown in Fig. 6. For waste heat at 140°C (284°F) and a condensing temperature of 70°C (158°F), the dilute solution flow rate (curve 2) for the two fluids is almost identical in the region of overlap. The refrigerant flow rate (curve 1) is slightly higher for the TNMs than it is for LiBr, and this explains why the absorber capacity, Q_A (curve 3), is also higher. The same behavior is obtained for a different set of waste heat 105°C (221°F) and condensing water 55°C (131°F) conditions as shown in Fig. 7.

As mentioned earlier, the primary purpose of focusing attention on the ternary nitrate mixtures is because they have the potential to operate at up to 260°C (500°F) with minimal corrosion of mild steel.

4.2 EFFECT OF SOLUTION HEAT EXCHANGER UA ON COP OF TNM

It is well-known that the coefficient of performance of a heat pump is sensitive to the effectiveness of the solution heat exchanger, other things being equal.[8] The effectiveness increases with the heat exchange surface area. Figure 8 shows the improvement in COP by increasing the surface area in the solution heat exchanger from 7.74 m^2 to 17.0 m^2. The waste heat source and cooling water temperature are 140°C (284°F) and 70°C (158°F), respectively. The COP increases by approximately 32% from its value of 0.31 corresponding to a solution heat exchanger area of 7.74 m^2. Figure 9 shows what effect the change in solution heat exchanger has on the refrigerant and dilute solution flow rates and the absorber heat release.

The most dramatic change is observed in the dilute solution flow rate as the solution heat exchanger area is increased from 7.74 m^2 to 17.0 m^2. The pure refrigerant too decreases, but the decrease is less than 10%. The significance of this is that the concentration difference between the concentrated and dilute solutions is greater when $A = 7.74\ m^2$ than it is when $A = 17.0\ m^2$.

The change in solution heat exchanger area also influences the total quantities of heat delivered to the evaporator and desorber and that rejected in the absorber. Since there is only a 10% change in the pure refrigerant flow rate, the heat input to the evaporator also changes in the same proportion. The desorber and absorber heat increases with increasing solution heat exchanger area. The net result is higher COP as shown in Fig. 8.

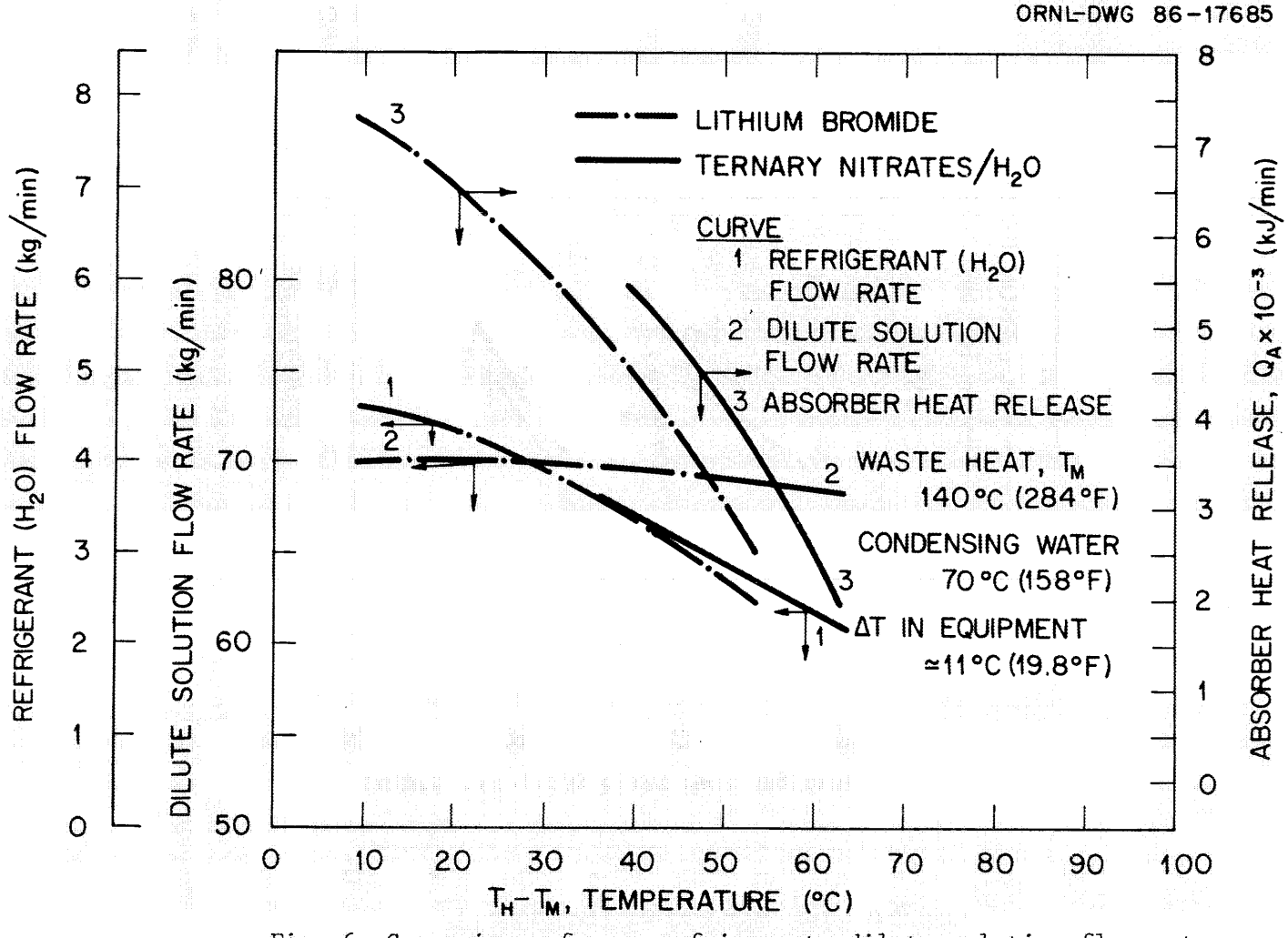

Fig. 6. Comparison of pure refrigerant, dilute solution flow rate and absorber heat release for LiBr and ternary nitrate mixtures.

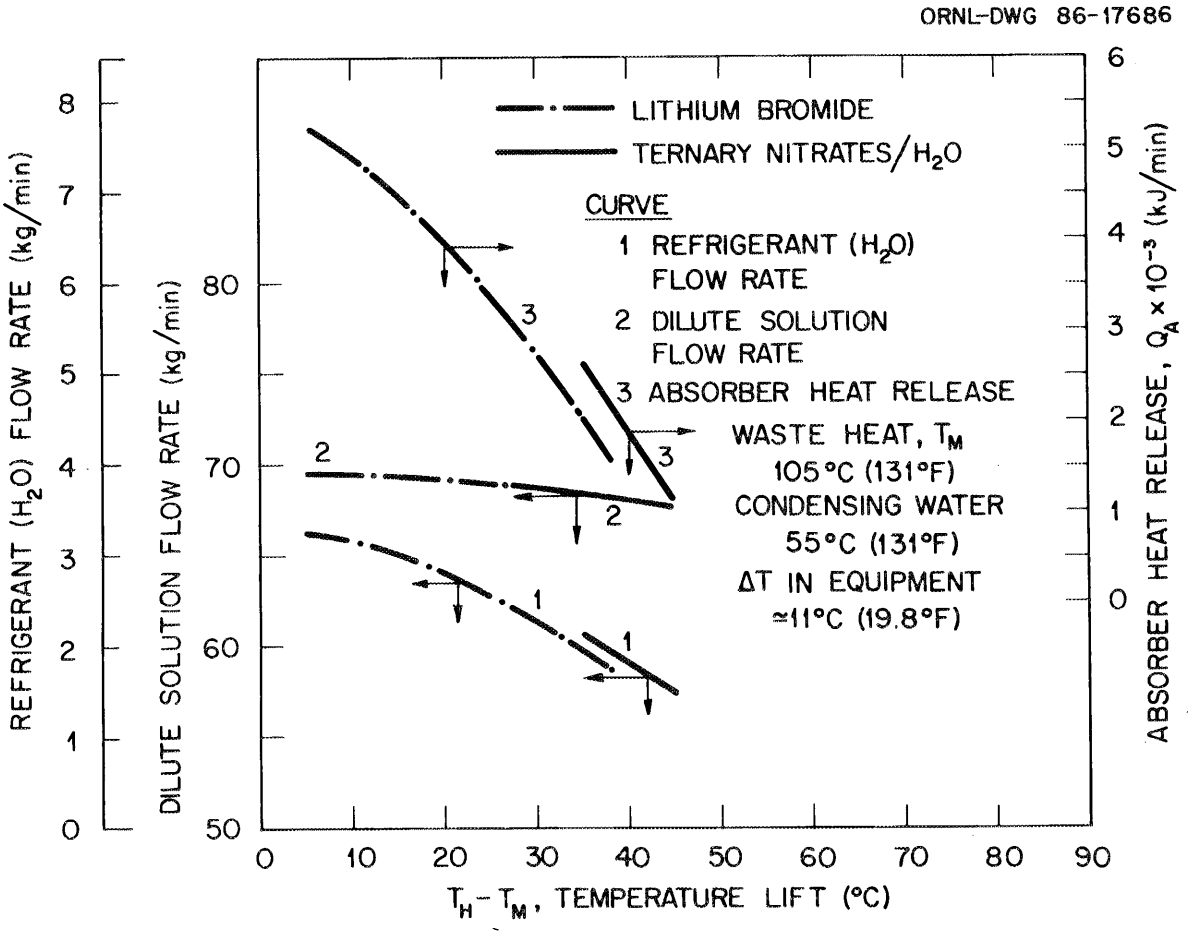

Fig. 7. Comparison of pure refrigerant, dilute solution flow rate and absorber heat release for LiBr and ternary nitrate mixtures.

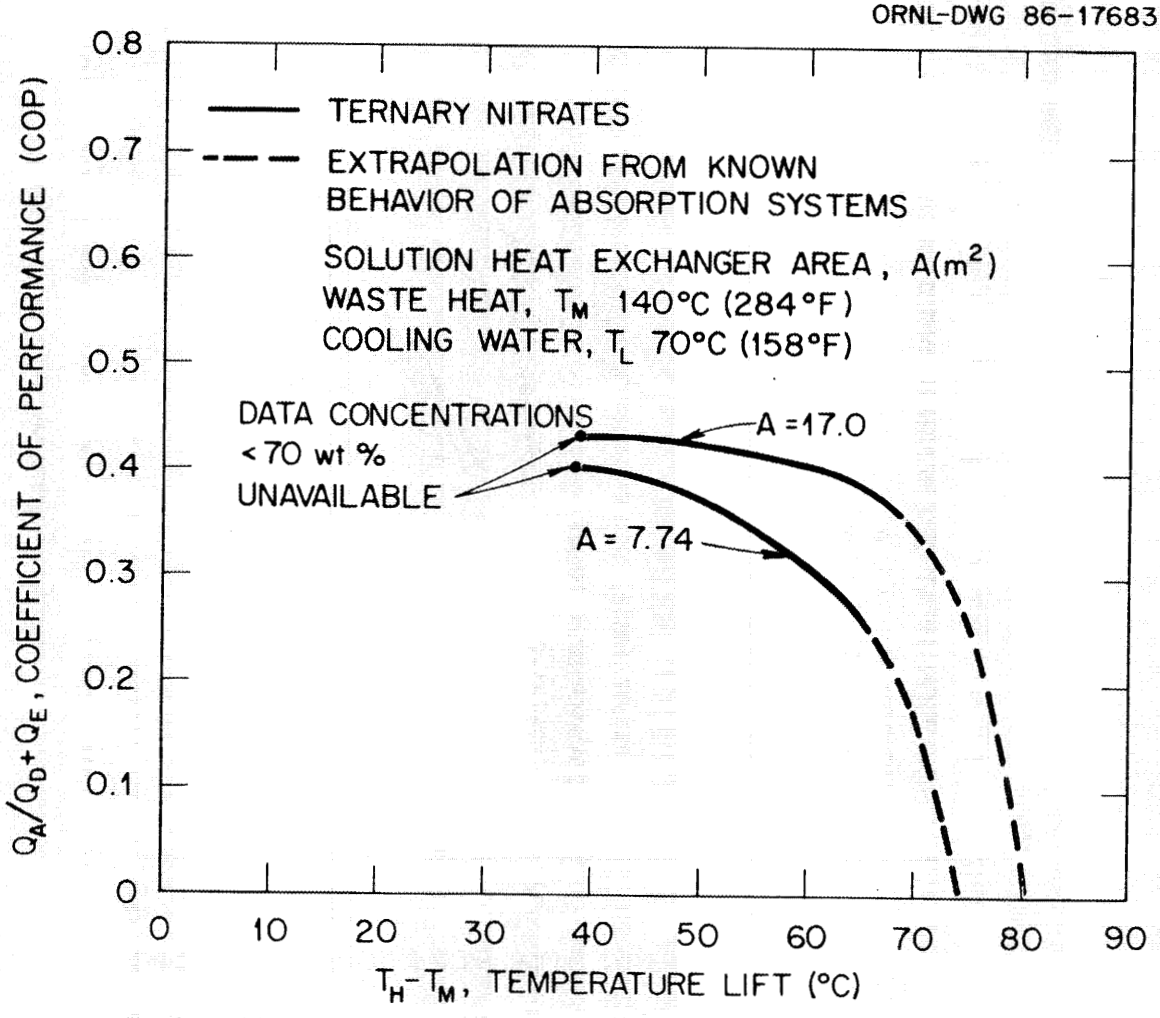

Fig. 8. Effect of increasing solution heat exchanger surface area on COP for ternary nitrate mixtures.

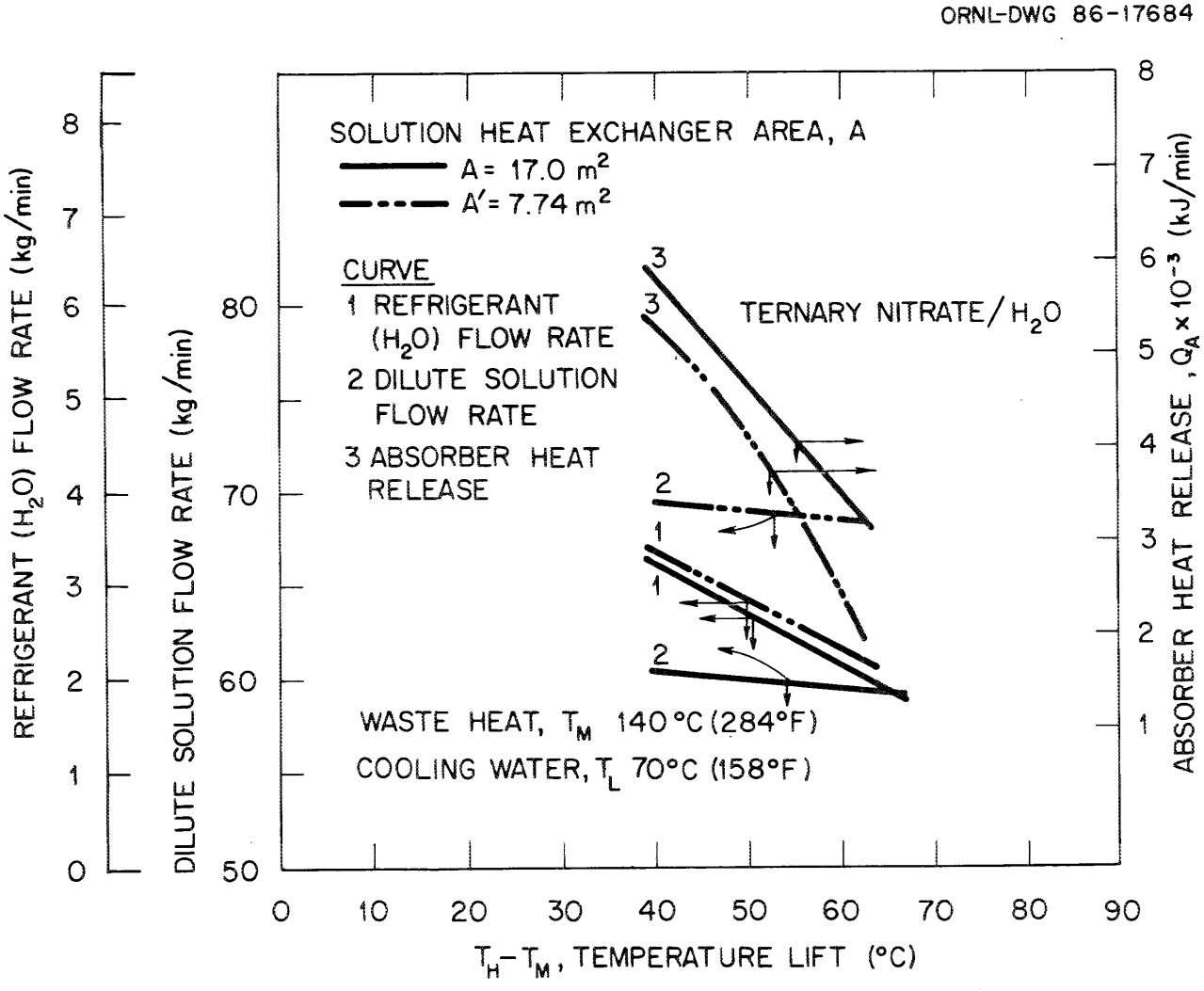

Fig. 9. Effect of increasing solution heat exchanger surface area on flow rate for ternary nitrate mixtures.

The computer simulation did not yield satisfactory results in the region of maximum attainable lift. This region is synonymous with the condition that the difference in concentration between the dilute and concentrated stream approach zero. Convergence in this particular region was not possible even when several different data sets were used. However, this limitation was not very discouraging because the behavior of absorption systems as the lift approaches its maximum value is well characterized. Improvement in existing software in this regard would be welcome.

4.3 INFLUENCE OF ABSORBER UA ON PERFORMANCE

In the case of the TNM, it has been discussed in Sect. 3 that the film heat transfer coefficient is expected to be about one-half that for LiBr. Taking this matter into consideration, the absorber UA is varied from its value in the prototype unit (114.21 W/K) to one-half (57.10 W/K) and down to one-third (38.07 W/K) for the TNM. Note that a 50% decrease in the film heat transfer coefficient, h_o, does not mean that the overall heat transfer coefficient, U, will also decrease by 50%. The actual decrease in U depends upon the magnitudes of the other heat transfer resistances in relation to each other, but since h_o is limiting, its influence on U is dominant. For the simulation, it is easier to deal with U directly than it is to deal with h_o and, hence, UA is varied.

The effect on performance of the anticipated decrease in h_o for the ternary nitrate is shown in Fig. 10, along with the curves for equal UAs. At lifts below 40°C (boost temperature <180°C), the ternary nitrate concentration falls lower than 70 wt %, for which data are unavailable. Lithium bromide at these lifts shows adequate performance with a COP of 0.4, although at 180°C boost temperature, the fluid is pushed to the limit (in the published literature) of upper-temperature applicability. At lifts greater than 40°C (boost temperature > 180°C), the COPs and the absorber heat release of the TNM are significantly higher than those of LiBr, even though the absorber UA for the TNM is half the value than for LiBr. The gap between the two fluids widens even further in favor of TNM as the lift is increased. The higher concentration of TNM has prompted researchers[9] to believe that the film heat transfer coefficient could be even lower. To incorporate their view, the absorber UA was decreased to one-third that for LiBr; the simulated results for the two competitor fluids are shown in Fig. 11. Once again, for lifts ≤40°C, LiBr has a higher COP than TNM, but in the region of higher lifts (>40°C), TNM still has a higher COP and marginally higher absorber capacity than LiBr.

The conclusions to be drawn from Figs. 10 and 11 are that (i) LiBr has a higher COP than TNM for lifts below 40°C provided that the boost temperature is sufficiently low (<177°C) to avoid corrosion problems, (ii) TNM is potentially capable of better COPs and higher quantities of

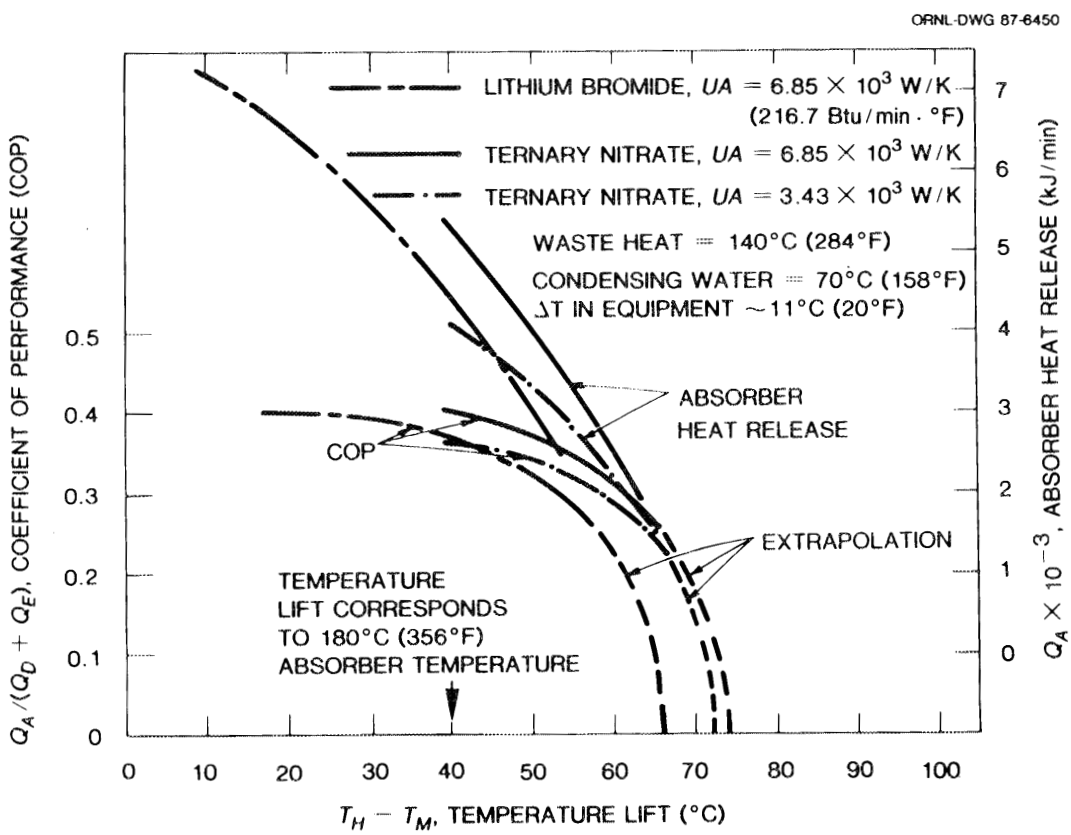

Fig. 10. Comparison of COP-lift and absorber heat release when absorber UA for ternary nitrate is one-half that of LiBr.

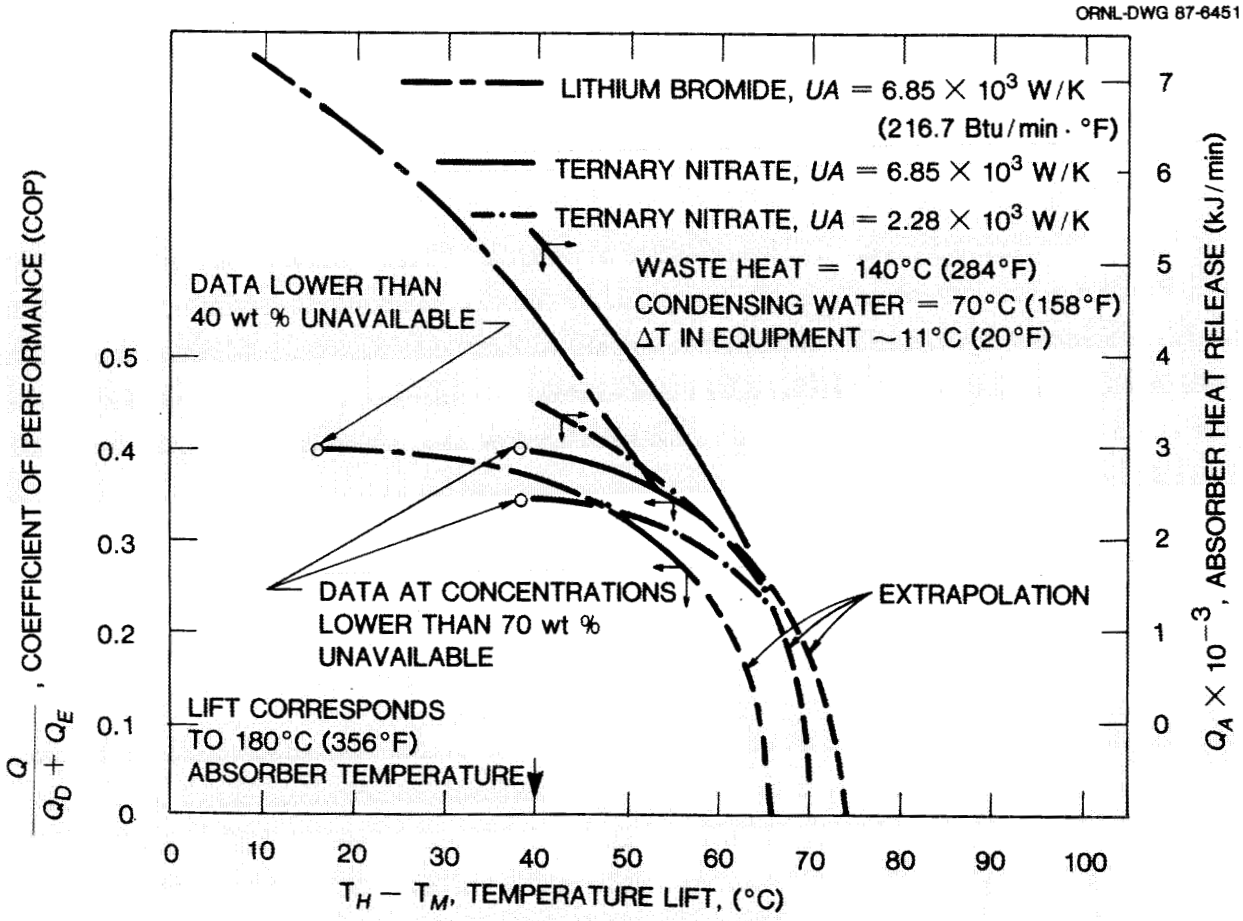

Fig. 11. Comparison of COP-lift and absorber heat release when absorber UA for ternary nitrate is one-third that of LiBr.

heat release through the absorber at lifts greater than 40°C and high boost temperature using waste heat at 140°C (284°F) even when the absorber UA is assumed as low as one-third its value for LiBr, and (iii) the film heat transfer coefficient is a strong determinant of the performance and needs to be known accurately.

5. CONCLUSIONS

The aqueous ternary nitrate mixture containing a solute composition of 53 wt % $LiNO_3$, 28 wt % KNO_3, and 19 wt % $NaNO_3$ is investigated for high-temperature (200-260°C) heat pump application. The nitrate mixture appears to have better COP, temperature lift, and absorber capacity capabilities than LiBr in the high-temperature range, even when the absorber overall heat transfer coefficient is reduced to one-third the value for LiBr. In lower-temperature lift regimes, the ternary nitrates are not competitive with LiBr. The strong point in favor of the nitrate mixtures is that they show the capability of operating about 80°C higher in temperature than has been published for LiBr.

Lack of thermophysical data for both fluids in the higher-temperature (>100°C) range proved a handicap overcome by extrapolation. A need for measuring thermophysical and corrosion properties is definitely required in future investigations for both fluids.

The absorber film heat transfer coefficient and the extent of subcooling are critical pieces of information which must be measured experimentally to quantify accurately the advantage that one fluid has with respect to the other in the temperature regimes of interest.

REFERENCES

1. B. A. Phillips, "Analysis of Advanced Residential Absorption Heat Pump Cycles,", *Proceedings of the DOE/ORNL Heat Pump Conference, Research and Development on Heat Pumps for Space Conditioning Applications, Washington, D.C., Dec. 11-13, 1984*, ORNL/CONF-841231, Oak Ridge National Laboratory, August 1985.

2. F. C. Hayes and R. J. Modahl, "Evaluation of Advanced Design Concepts for Absorption Heat Pumps," *Proceedings of the DOE/ORNL Heat Pump Conference, Research and Development on Heat Pumps for Space Conditioning Applications, Washington, D.C., Dec. 11-13, 1984*, ORNL/CONF-841231, Oak Ridge National Laboratory, August 1985.

3. W. F. Davidson and D. C. Erickson, *New High Temperature Absorbent for Absorption Heat Pumps*, ORNL/Sub/85-22013/1, Energy Concepts Company, Annapolis, Maryland, July 1986.

4. ASHRAE, *1985 Fundamentals*, American Society of Heating, Refrigeration, and Air-Conditioning Engineers, pp. 17.71-17.72.

5. M. R. Ally, *Thermodynamic Properties of Aqueous Ternary Solutions Relevant to Chemical Heat Pumps*, ORNL/TM-10258, Oak Ridge National Laboratory (1987).

6. G. Grossman and E. Michelson, *Absorption Heat Pump Simulation and Studies, Part 1: A Modular Computer Simulation and Absorption System*, ORNL/Sub/83-43337/?, Oak Ridge National Laboratory, December 1985.

7. Eckhart Blab, *Chem.-Ing.-Tech.* **49**(2), 95-105 (1977).

8. H. Perez-Blanco and G. Grossman, *Cycle and Performance Analysis of Absorption Heat Pumps for Waste Heat Utilization*, ORNL/TM-7852, Oak Ridge National Laboratory, September 1981.

9. W. Biermann, Personal Communications.

10. R. C. DeVault, Personal Communications.

APPENDIX

Estimation of film heat transfer coefficients

a) Aqueous Lithium Bromide Mixtures

Waste heat = 140°C (284°F)
Absorber solution temperature ≈ 180°C (356°F)
Average solution concentration = 60% by weight

Viscosity (Fig. 2c), $\mu \approx 1.5$ mPa·s
Specific gravity (Fig. 2d), ≈ 1.63
Density, $\zeta \approx 1.63 \times 55.37 \times 16.018 = 1446$ kg/m³

Kinematic viscosity, $\nu = \frac{\mu}{\zeta} = 1.038 \times 10^{-6}$ m²/s

Film thickness, $\delta = \left(\frac{3\nu^2}{g}\right)^{1/3} (Re)^{1/3}$

Typical Reynolds Number, Re ≈ 100

Therefore, $\delta = 3.206 \times 10^{-4}$ m

Thermal conductivity of stated solution (Fig. 2e) ≈ 0.51 W/m·K

Film heat transfer coefficient, $h = \frac{k}{\delta} = 1591$ W/m²·K
h = 1591 W/m²·K at ≈ 180°C, 60 wt %

b) Aqueous Ternary Nitrate Mixtures

Waste Heat = 140°C (284°F)
Absorber solution temperature ≈ 180°C (356°F)
Average solution concentration ≈ 78% by weight

Viscosity (Fig. 2c), $\mu \approx 2.5$ mPa·s
Density (ref. 3, p. 23), $\zeta \approx 1.63$ g/cm³ = 1.63×10^3 kg/m³

Kinematic viscosity, $\nu = \frac{\mu}{\zeta} = 1.534 \times 10^{-6}$ m²/s

Film thickness, $\delta = \left(\frac{3\nu^2}{g}\right)^{1/3} (Re)^{1/3}$

Typical Reynolds Number, Re ≈ 100

Therefore, $\delta = 4.159 \times 10^{-4}$ m

Thermal conductivity of stated solution ≈ 0.33 W/m·K

Film heat transfer coefficient, $h = \frac{k}{\delta} = 793.4$ W/m²·K
h = 793.4 W/m²·K at ≈ 180°C, 78 wt %

INTERNAL DISTRIBUTION

1-5. M. R. Ally
6. V. D. Baxter
7. R. B. Braid
8. R. S. Carlsmith
9. F. C. Chen
10. F. A. Creswick
11. R. C. DeVault
12. N. Domingo
13. P. D. Fairchild
14. F. G. Farrell
15. S. K. Fischer
16. W. Fulkerson
17. M. B. Gettings
18. I. G. Harrison
19. R. O. Johnson
20. J. O. Kolb
21. M. A. Kuliasha
22. R. S. Loffman
23. F. C. Maienschein
24. J. F. Martin
25. H. A. McLain
26. V. C. Mei
27. D. R. Miller
28. M. Olszewski
29. H. Perez-Blanco
30. E. T. Rogers
31. A. C. Schaffhauser
32. B. K. Seivers
33. R. B. Shelton
34. J. J. Tomlinson
35. C. D. West
36. T. J. Wilbanks
37. Central Research Library
38. Document Reference Section
39-43. Energy Conservation Dist. Bldg. 9102-2, Room 103
44-46. Laboratory Records
47. Laboratory Records - RC
48. ORNL Patent Office

EXTERNAL DISTRIBUTION

49. W. J. Biermann, 45 Foxcroft Drive, Fayetteville, NY 13066

50. J. M. Calm, Electric Power Research Institute, P.O. Box 10412, Palo Alto, CA 94303

51. J. G. Carbonell, Associate Professor of Computer Science, Carnegie-Mellon University, Pittsburgh, PA 15213

52. G. Douglas Carver, Tennessee Valley Authority, 703 Power Building, Chattanooga, TN 37402

53. R. N. Chappell, Idaho Operations Office, U.S. Department of Energy, 785 DOE Place, Idaho Falls, ID 83402

54. D. C. Erickson, Energy Concepts Co., 627 Ridgely Avenue, Annapolis, MD 21401

55. R. J. Fiskum, Program Manager, Energy Conversion Equipment Branch, CE-132, Room GF-217/FORS, U.S. Department of Energy, 1000 Independence Avenue SW, Washington, DC 20585

56. J. Gilbert, Dames & Moore, Inc., 7101 Wisconsin Avenue, Suite 700, Bethesda, MD 20814

57. S. M. Gillis, Dean, Graduate School, Duke University, 4875 Duke Station, Durham, NC 27706

58. G. Grossman, Technion-Israel Institute of Technology, Faculty of Mechanical Engineering, Haifa, Israel

59. W. T. Hanna, Battelle Columbus Laboratories, 505 King Avenue, Columbus, OH 43201

60. F. C. Hayes, Trane Company, 3600 Pammel Creek Road, LaCrosse, WI 54601

61. F. R. Kalhammer, Vice President, Electric Power Research Institute, P.O. Box 10412, Palo Alto, CA 94303

62. A. Karp, Energy Management & Utilization Division, Electric Power Research Institute, 3412 Hillview Avenue, Palo Alto, CA 94303

63. R. E. Kasperson, Professor, Government and Geography, Graduate School of Geography, Clark University, Worcester, MA 01610

64. R. Macriss, Institute of Gas Technology, 3424 South State Street, Chicago, IL 60616

65. L. A. McNeely, 7310 Steinmeier Drive, Indianapolis, IN 46250

66. D. K. Miller, Borg-Warner Air Conditioning Inc., P.O. Box 1592, York, PA 17405

67. J. I. Mills, EG&G-Idaho Inc., P.O. Box 1625-WCB, Idaho Falls, ID 83415

68. R. L. Perrine, Professor, Engineering and Applied Science, Civil Engineering Department, Engineering I, Room 2066, University of California, Los Angeles, CA 90024

69. B. A. Phillips, Phillips Engineering Co., 721 Pleasant Street, St. Joseph, MI 49085

70. R. Radermacher, University of Maryland, Department of Mechanical Engineering, College Park, MD 20742

71. R. C. Reinmann, Carrier Corp., P.O. Box 4808, Syracuse, NY 13221

72. S. L. Richlen, Office of Industrial Programs, CE-141, 5F-035/FORS, U.S. Department of Energy, 1000 Independence Avenue SW, Washington, DC 20585

73. U. Rockenfeller, Rocky Research Company, 1453 Rawhide Road, Boulder City, NV 89005

74. J. D. Ryan, Office of Buildings and Community Systems, CE-132, GF-217/FORS, U.S. Department of Energy, 1000 Independence Avenue SW, Washington, DC 20585

75. D. S. Severson, Gas Research Institute, 8800 West Bryn Mawr Avenue, Chicago, IL 60631

76. S. V. Shelton, Department of Mechanical Engineering, Georgia Institute of Technology, Atlanta, GA 30332

77. J. J. Tuzson, Gas Research Institute, 8800 West Bryn Mawr Avenue, Chicago, IL 60631

78. G. C. Vliet, Taylor Hall 116, University of Texas, Austin, TX 78712

79. M. Wahlig, Lawrence Berkeley Laboratory, University of California, Berkeley, CA 94720

80. Office of Assistant Manager for Energy Research and Development, DOE-ORO, Oak Ridge, TN 37830

81-90. OSTI, U.S. Department of Energy, P.O. Box 62, Oak Ridge, TN 37830